A transient method for characterizing flow regimes in a circulating fluid bed

Esmail R. Monazam[a], Lawrence J. Shadle[b,*]

[a] REM Engineering Services, PLLC, 3537 Collins Ferry Rd., Morgantown, WV 26505, USA
[b] National Energy Technology Laboratory, U.S. Department of Energy, 3610 Collins Ferry Rd., Morgantown, WV 26507-0880, USA

Abstract

In recent years, although an increasing number of literature have been devoted to circulating fluidized bed (CFB), the prediction of velocities over which different fluidization regimes exist is still difficult. In this study, a transient method was applied which readily allows one to identify operational features and critical transitions. The method is based on stopping the solids flow rate into the riser when riser is operating in fully dense transport regime. The analysis of transient pressure drop data across the riser during a solids flow cut-off experiment against its time derivative demonstrate the three distinct operating regimes that exist as the gas deplete the solid out of the riser. The transient was compared to data taken under steady state operations using statistically designed experiments. Results indicated that although there were significant differences when comparing operations in dilute conditions, there were no significant differences between the two methods in the fast fluidized and dense transport regimes. The transient method was capable of reproducing the solids circulation dependence on riser solids holdup and on the axial pressure profile. This transient method offers an accurate, easy, rapid, and reproducible means of characterizing CFB operations over a wide range of flow conditions. The lack of accuracy in the dilute regime is conjectured to be due to the wide particle size distribution that resulted in segregation during the transient testing.

1. Introduction

Circulating fluidized beds (CFB) and pneumatic conveying of solids have been widely used in chemical and petroleum industries, including pressurized circulating fluidized bed combustion, catalytic cracking, and aluminum oxide calcination. Understanding of the flow regimes in CFB risers is the key to successful design and scale-up of CFB systems. Numerous studies on CFB riser's regimes are available in the literature [1–6]. Due to the restricted range of operating conditions, generally, these studies are carried out for the specific regimes (i.e., dilute, fast fluidized, and dense). For instance, studies on the dilute regime do not provide any information on the neighboring regimes such as fast fluidized regime. Therefore, it is difficult to recognize the operating conditions for fast fluidized regime. There is a lot of controversy in the literature on the actual events occurring in different flow regimes and even the definition of transport velocity [7]. In this paper, the transport velocity is defined according to Yerushalmi and Cankurt [1] as the velocity at which it is possible to transfer all of the solids introduced into the riser, and thus it is impossible to maintain a fluidized bed without continuous recycle of solids back into the fluid bed. This is the critical gas velocity defining the transition between turbulent and fast fluidized flow regimes. For example, Yerushalmi and Cankurt [1] studied the effect of gas velocity and solids circulation rate on the pressure gradient for fluid bed operations below the transport velocity. With an increase in solid flow rate, they found a sharp transition between dilute-phase flows and nonslugging dense flow. This transition is illustrated by a sharp increase in the pressure gradient for a given gas velocity. Operation of a CFB between the fully dilute- and the fully dense-phase flow regimes was reported to be unstable when operating below the transport velocity.

Bai and Kato [8] made experimental observations that suggest that the solids move cocurrently upward with the gas in dilute pneumatic transport at a very low solids flow

* Corresponding author. Tel.: +1-304-285-4647; fax: +1-304-285-4403.
E-mail address: lshadl@netl.doe.gov (L.J. Shadle).

rate for any gas velocity. As solids flow increases beyond the dilute-phase flow regime, a relative dense bed forms at the bottom of the riser. Solids begin to accumulate at the bottom of the riser, and a typical S-shaped solid holdup distribution starts to form. Further increasing the solids flow rate has no effect on solids holdup in the dense region; it only causes growth of the height for the dense region as the interface between the dense and dilute region rises up the riser. If there is enough solids inventory available in the system, an increase in solids flow rate results in eventually completely filling the riser with a dense bed. As opposed to Yerushalmi and Cankurt's observations [1], stable operations are implicitly observed throughout this regime. Although unstated, this apparently takes place at gas velocities above Yerushalmi's transport velocity.

According to the theoretical analysis by Li et al. [9], the S-shaped axial voidage profile represents the critical state for choking, and whenever the S-shaped profile appears for a given gas velocity, the corresponding solids flow rate is bound to be equal to the saturation carrying capacity (SCC). At this point, an increase in the gas velocity collapses the S-shaped axial voidage profile into a single dilute flow. On the other hand, an increase in solids flow rate causes the S-shaped axial voidage profile to grow into a dense bed of uniform voidage. In a state where the S-shaped axial voidage profiles exist, the solid inventory is known to affect the axial profile.

Thus, the literature includes description of various transitions across different regimes without common reference points or definitions. Therefore, there is considerable confusion in the literature regarding the gas–solid flow, the transitions between various regimes, and the actual characteristics in different flow regimes.

In this study, a new transient method is presented to characterize the different flow regimes and identify the transition between each regime. The method is based on transient pressure drop measurement across the riser during a solids flow cut-off experiment while maintaining constant gas flow. This method is a rapid means of mapping the relationships between pressure profiles, gas velocity, and solids flux for a given material.

2. Experiment

The test unit configuration is described by Monazam et al. [10] and shown in Fig. 1. The riser is constructed of flanged steel sections with one 1.22 m acrylic section installed 2.44 m above the solids feed location. The solids enter the riser from a side port 0.23 m in diameter and 0.27 m above the gas distributor. Solids exit the riser through a 0.20 m port at 90° about 1.2 m below the top of the riser at a point 15.45 m above the solids entry location (centerline to centerline). Riser velocities were corrected for temperature and pressure as measured at the base of the riser. Twenty

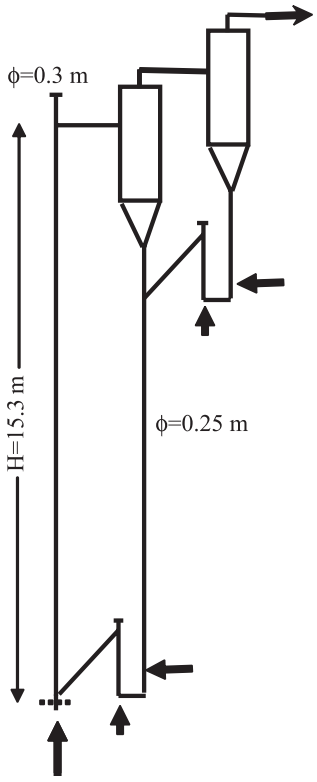

Fig. 1. Schematic of the NETL cold flow circulating fluid bed unit.

incremental differential pressures were measured across the length of the riser using transmitters calibrated within 0.1% of full scale or about 2 Pa/m. The other primary response measurement was the overall riser pressure differential, and it was calibrated within 0.45 Pa/m. Mass circulation rate was continuously recorded by measuring the rotational speed of a twisted spiral vane located in the packed region of the standpipe bed [11]. This calibrated volumetric measurement was converted to a mass flux using the measured packed bed density, presented in Table 1, and assuming that the void fraction at the point of measurement is constant. Analysis of the standpipe pressure profile, estimated relative gas–solids velocities, and bed heights have indicated that this constant voidage estimate is reasonable over the range of operating conditions reported here. The solids circulation was varied by controlling the aeration at the base of the standpipe and by adjusting the total system inventory to increase the standpipe height. Steady state conditions were defined as holding a constant set of flow conditions and maintaining a constant response in the pressure differentials over a 5-min period. All steady state test results represent an average over that 5-min period. During an experiment, the air velocity in the riser was controlled at a constant level. The superficial riser velocity was the summation of the flow at the base of the riser with that at the base of the lift-leg in the loopseal.

In this study, the bed material used was cork. The material properties are presented in Table 1. This is a Geldart Type A granular material. In order to avoid

Table 1
Bed material properties

Cork characteristics		
ρ_s	kg/m^3	189
ρ_b	kg/m^3	95
ε_b		0.45
d_{p50}	μm	1170
d_{sv}	μm	812
U_t	m/s	0.86
U_{mf}	m/s	0.17
ε_{mf}		0.49
ϕ		0.84

interference due to static charge, the air relative humidity was maintained at about 40% by introducing steam when necessary.

3. Results and discussion

A review of literature concerning the different flow regime in circulating fluidized bed (CFB) suggested that: the dilute transport regime is characterized as a uniform void fraction along the vertical axes of the riser in circulating fluid bed (CFB). By increasing the solids flux for a given gas velocity, the solids tend to fall in denser clusters along the wall and rise in more dilute concentrations towards the center, producing a core–annular flow. The onset of fast fluidization is observed when the solids flux is increased to the point of saturation carrying capacity (G_s^*) [9,10]. At this point, a dense-phase transport region forms in the lower regions below a dilute-phase transport region in the upper part of the riser. The fully developed fast fluidized bed regime exhibits a gradual transition between the lower dense bed and the upper dilute bed that has been described as an either S-shaped profile [12] or a simple exponential profile [13] in solid concentration along the length of the riser. By increasing the solid inventory into the riser, the inflection point in the axial voidage profile moves upward until it passes beyond the top of the bed. As the dense bed approaches the top of the bed, the onset of fully dense flow regime is observed. This regime is characterized according to Li [14] as particle-fluid compromising (PFC). The voidage profile in PFC regime is constant and covers ranges between 0.75 and 0.9 [15].

In this study, we have undertaken a series of transient experiments to characterize these different flow regimes. For this purpose, while the riser of CFB was operated at a steady state condition within the PFC regime above Yerushalmi and Cankurt's transport velocity [1], the solids circulation rate was abruptly stopped. This was accomplished by diverting the flows being introduced into the base of the standpipe (the move air) to the atmosphere. After this solids flow cutoff, the pressure gradient across the entire riser and 23 incremental pressure drops along the riser were recorded as a function of time. These pressure drops were recorded as a function of time at a sampling rate of 1 Hz. As the solids inventory was carried out of the riser, the pressure drop across the riser decreased. As expected, an increase in the gas velocity decreased the time required to empty the bed. These measurements are useful for determining the different flow regimes and the transition between each regime for the corresponding gas velocity.

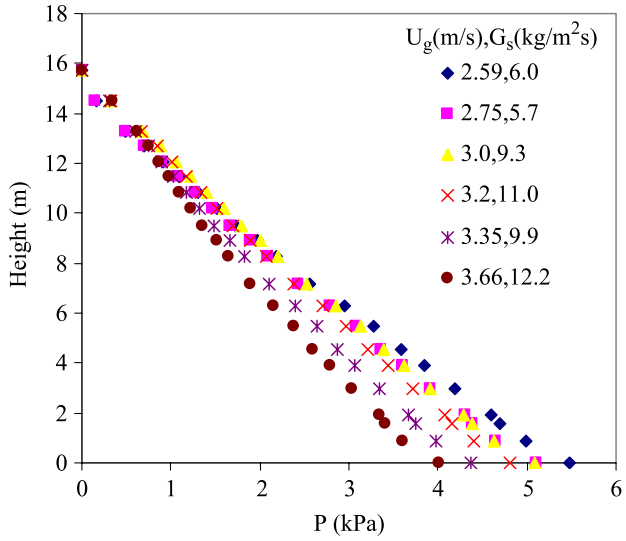

Fig. 2. Steady state, time-averaged (5 min), pressure profiles along the riser in dense transport for different operating condition (U_g and G_s).

The axial pressure drop profiles along the riser of CFB during steady state operations are displayed in Fig. 2 for different superficial gas velocities and solid mass fluxes. In fully dense riser, the observed incremental pressure gradient

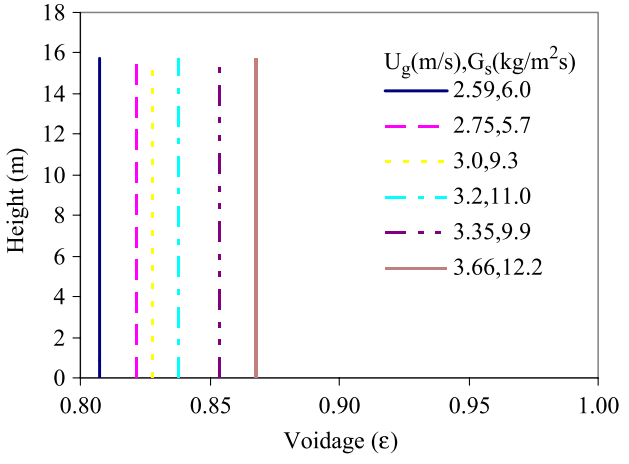

Fig. 3. Steady state axial voidage profiles as a function of gas velocity when operating in the dense transport regime.

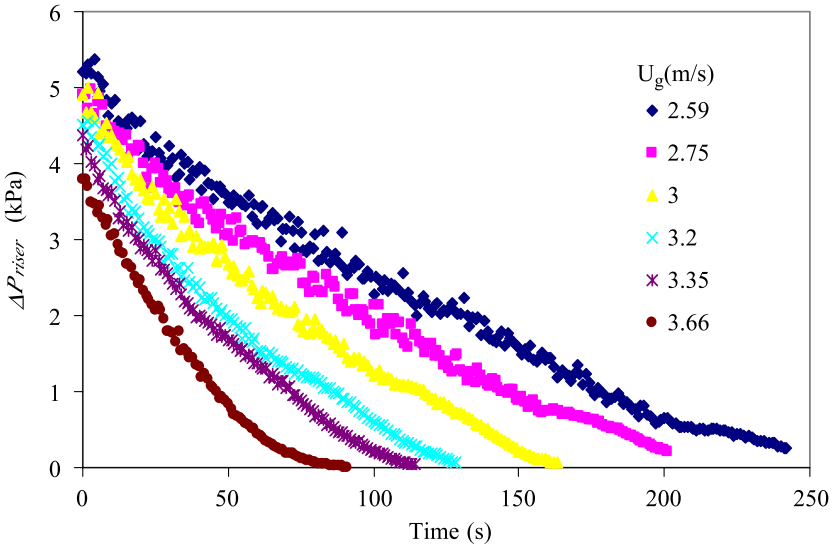

Fig. 4. Decay profile for overall riser pressure drop (ΔP_{Riser}) after halting solids flow for different gas velocities (U_g).

across the riser was linear (Fig. 2). Steady state operation was determined when the average riser pressure profile was constant for 5 min. The axial voidage profiles are shown in Fig. 3 as computed from the corresponding differential pressure drop, assuming there is a negligible contribution of acceleration and wall friction [16]. The axial voidage profiles clearly provided evidence that the riser was operating in fully dense (PFC) regime with constant voidage. The voidage profile was constant with values ranging between 0.80 and 0.87; the voidage increased with the increasing of gas velocity. This is typical of a riser operated in the PFC regime.

To evaluate the solids flux during this transient (during the emptying time), the pressure drop across the riser (Fig. 4) was fitted to a polynomial in time (6th order) and then differentiated ($d\Delta P_{\text{Riser}}/dt$). During the transient, the solids flux leaving the riser at any time, t, was obtained as described by Monazam et al. [10]:

$$G_s(t) = -\frac{1}{g}\frac{d\Delta P_{\text{Riser}}}{dt} \tag{1}$$

The solids flux leaving the riser during the emptying process is presented in Figs. 5 and 6 for different gas velocities as a function of ΔP_{Riser} and voidage. The average voidage during the emptying time was obtained using the pressure drop across the riser for a given time through the following expression [16]:

$$\frac{d\Delta P_{\text{Riser}}}{dz} = \rho_s(1-\varepsilon)g \tag{2}$$

Stopping the solids flow rate into the riser when riser is operating in PFC or fully dense regime demonstrates three

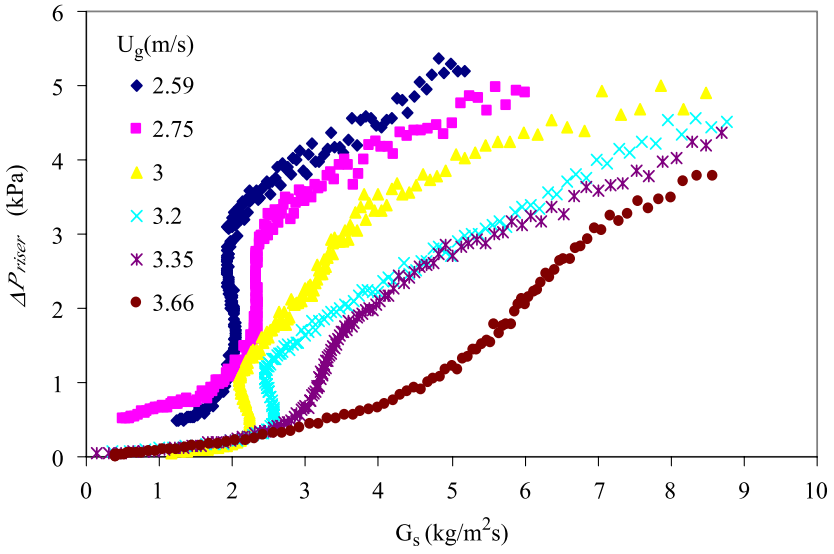

Fig. 5. Operating map for cork using $\Delta P/\Delta L - G_s - U_g$ plot developed by Yerushalmi and Cankurt [1]. Pressure drop reported as taken over total riser length.

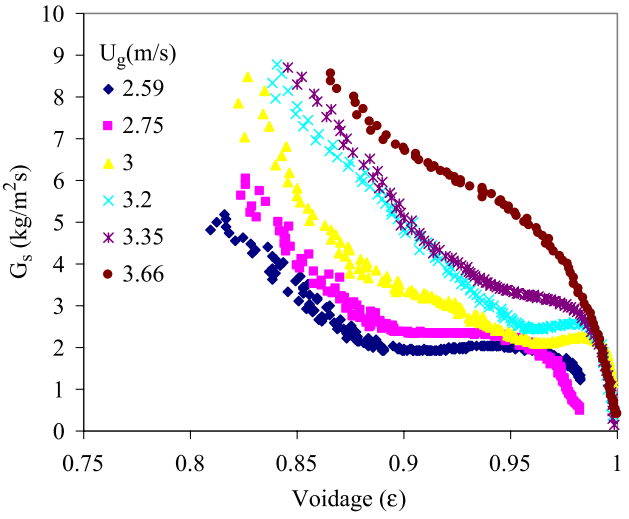

Fig. 6. Transient decay profile over a range of gas velocities (U_g) for solids flux from Eq. (1) as a function of average riser voidage from Eq. (2).

distinct modes of operation that exist as the gas depletes the solids out of the riser (Figs. 5 and 6). Three linear regions in these transient ΔP decay curves are very clear for the lower velocities ($U_g = 2.59$ and 2.75 m/s). Initially, after the solid cutoff, the ΔP_{Riser} decreased from its maximum value linearly with solid flux until the onset of fast fluidization ($G_s \approx 2$ kg/m^2 s). At this point, the solid flux remained constant while ΔP_{Riser} decreased. The riser inventory then approached the point where the constant solids flux was supported and the onset of the dilute regime was observed. In the dilute regime, both ΔP_{Riser} and solid flux decreased as the solid inventory leave the riser. These phenomena are demonstrated in Fig. 7 where the calculated axial voidage profile is portrayed along the riser during the emptying time. The voidage profiles clearly provide evidence that the riser progressed from fully dense to fully dilute regimes. The profiles taken during constant solids flux period were clearly S-shaped voidage profiles characteristic of the fast fluidization regime.

In Fig. 5, there was a clearly identifiable transition velocity between $U_g = 3.35$ and 3.66 m/s above which S-shaped voidage profiles were not observed for any given solids flux. This was not the transport velocity as defined by Yerushalmi and Cankurt [1], rather this was the velocity demarking the transition from the fast fluidized bed to the core–annulus dilute regime. This velocity compared favorably with the transition velocity in the plot of emptying time against the gas velocity for cork material (Fig. 8) using the method described by Perales et al. [17]. Their method was developed for the transition between bubbling and fast fluid bed regime; however, the measurement here was made for the transition between the fast fluid regime and the core-annulus dilute transport regime. This transition represented the upper limit in the velocity domain for type A choking, V_{CA} [6], or the SCC [10]. This transition velocity was interpreted to be the tip of the horizontally directed parabola in the $\Delta P/\Delta L - G_s - U_g$ plot presented by Wirth [18] and Shadle et al. [19]. The transition velocity in this study is the highest velocity that the S-shaped voidage profiles can be observed in the riser. For the purposes of this paper, the C-shaped profile was considered to be part of the core–annular regime. It is noted that at higher solids flux conditions, a C-shaped profile was generated above this upper transition velocity, but no S-shaped solid fraction profiles were observed. It must also be acknowledged that changes in the inlet or outlet configurations, riser diameter, or height may result in changes in this upper transition velocity.

The key features in the transient after halting the solid flow were independent of the initial steady state solids flux (Fig. 9). The solids holdup in the riser drops off gradually until the solids flux out of the riser reaches the saturated carrying capacity at which point the solids holdup drops sharply. As long as the riser is completely filled and operating in the dense transport regime, the initial solids

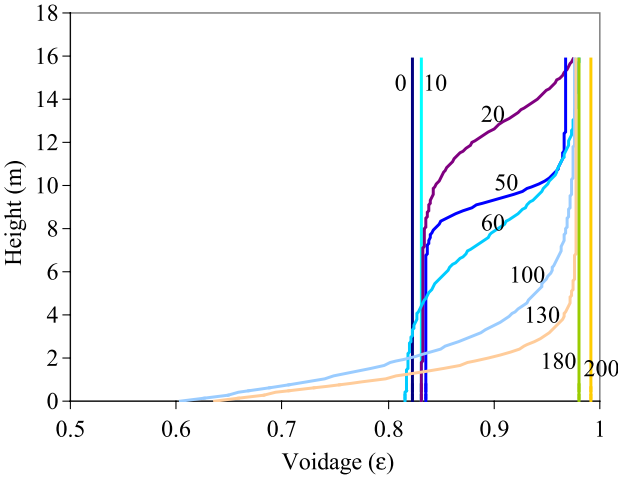

Fig. 7. Axial voidage profile along the riser as a function of time (s) after halting the solids flow, $U_g = 2.75$ m/s.

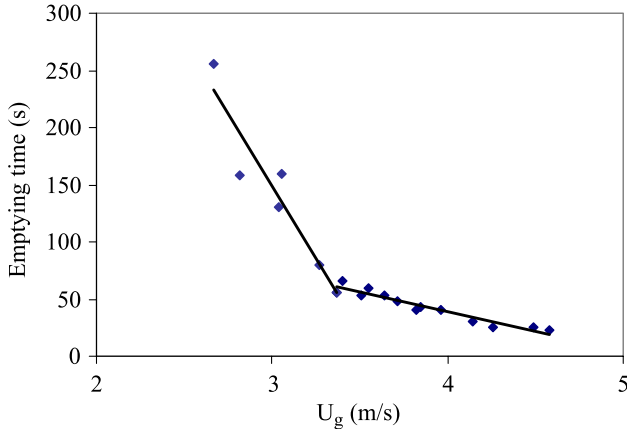

Fig. 8. Decay time method for estimating the transition velocity between fast fluidization and core–annulus/dilute transport regimes.

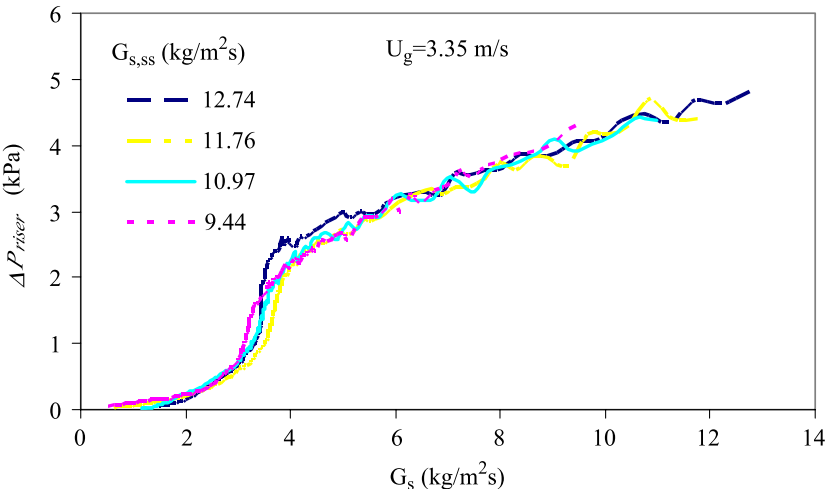

Fig. 9. The effect of altering the solids flux on the $\Delta P/\Delta L - G_s - U_g$ plot produced using the transient method.

flux did not affect the transient. The transient only depended upon the gas velocity; the saturation carrying capacity increased as the gas velocity increased. This trend agrees with that reported by Li et al. [9] and Monazam et al. [10]. This demonstrates that the initial solid flux neither influences the onset of the fast fluidization regime from the dense regime nor the onset of the dilute regime from the fast fluidization regime.

A series of transients and steady state measurements were taken to evaluate the reproducibility of the transients after solids cutoff, and further to make quantitative comparison between instantaneous responses within the transient with those measured under steady state conditions. The riser was operated at two gas velocities that were operated in each of the three regimes by varying the solids flux—the dilute, fast fluidized, and dense transport regimes. All of these tests were duplicated and were in randomized order to provide unbiased estimate of error. The transient tests were conducted immediately following the steady state condition with the highest solids flux because these were in the dense transport regime, and the time decay would then progressively pass through the fast fluidized and dilute regimes. The transient data was transformed to plot ΔP_{Riser} against the solids flux using Eq. (1) (Fig. 10). The duplicate transients are represented as different colored lines on this plot and were found to agree very closely to one another. In particular, both of the duplicates exhibited similar saturation carrying capacities, the vertical portions of the curve where the solids flux was constant over a wide range of ΔP_{Riser}.

In addition, each of the four steady state values and their duplicates are also displayed in Fig. 10 for each gas velocity, and these are represented as symbols. These duplicates agree very closely and are hardly distinguishable from each other on the plot. These points fall closely to the lines representing the transient for each gas velocity in the dense transport region, i.e., the higher solids fluxes. The solids

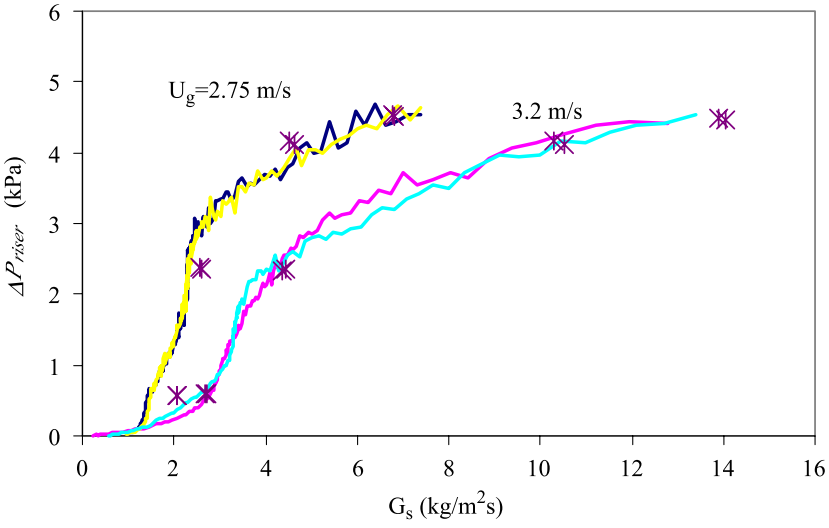

Fig. 10. Comparison of steady state, time-averaged (5 min), overall riser pressure drop (ΔP_{Riser}) with the associated total riser pressure decay transient at two gas velocities (U_g; see also Table 2).

flux where the ΔP_{Riser} drops off, corresponding to the SCC, was slightly lower for the transient data as compared to the steady state data. This difference between steady state and transient data was smaller at the higher gas velocity. The transition to dilute regime was observed at a lower solids flux using the transient method as compared to the steady state points. This was exaggerated for the lower gas velocity. This deviation may be due to the particle size and density segregation during the transient experiments considering that the larger, denser particles are the last particles entrained out of the riser. Thus, the higher velocity was less prone to such segregation and the transient data agreed closer with steady state data.

An Analysis of Variance (ANOVA) was conducted to statistically evaluate the significance of the independent parameters studied: U_g, ΔP_{Riser}, and test method (steady state vs. transient). For the steady state data analysis, there were two gas velocities and three levels of ΔP_{Riser}, and the same two gas velocities were tested for the transient method. In the transient method three solids flux values were determined for each test case corresponding to the three riser ΔP levels. When fully duplicated and randomized, this resulted in 16 conditions in which the solids flux (dependent parameter) was determined as described above. This data is presented in Table 2. The full set of data was compared using a general linear model including the main effects, secondary interactions ($U_g \times \Delta P_{Riser}$, $U_g \times$ method, $\Delta P_{Riser} \times$ method), and tertiary interactions ($\Delta P_{Riser} \times$ method $\times U_g$). The *F*-test indicated that there were significant differences for each of the main effects and the interactions. However, this was expected because a bias was observed between the methods at the lower flux and gas velocities likely due to segregation in this bed material that has been reported to have a wide size distribution [19]. For this reason, the ANOVA was redone for the two higher solids flux cases (Table 3). The *F*-test for this reduced data set indicated that the two methods (steady state vs. transient) were not significantly different (at 95% confidence level) for the determination of solids flux.

In addition, the three-way interaction was not a significant parameter in the ANOVA. However, the interaction between methods and both U_g and ΔP_{Riser} were significant. Again, this may be an example of residual effects of analysis of nonhomogeneous materials having a distribution of both size and density. Further testing is underway on a more narrowly sized uniform density bed material to confirm the results suggested here.

Table 2
Test results for statistically designed duplicated experiments to compare steady state and transient methods in sequence conducted

Method	U_g (m/s)	G_s (kg/m^2 s)	ΔP_{Riser} (kPa)
Transient	2.80	6.82	4.52
Steady state	2.80	4.52	4.16
Steady state	3.21	2.72	0.60
Steady state	3.20	10.29	4.16
Transient	3.20	13.90	4.49
Steady state	3.20	4.44	2.36
Steady state	2.80	2.59	2.37
Steady state	2.80	2.06	0.58
Steady state	2.81	2.57	2.37
Steady state	2.79	4.63	4.12
Steady state	3.20	2.67	0.59
Transient	2.79	6.78	4.53
Steady state	3.20	10.53	4.12
Steady state	2.80	2.05	0.58
Steady state	3.20	4.36	2.33
Transient	3.20	14.05	4.47

Table 3
ANOVA table comparing the estimate of G_s from a general linear model including riser gas velocity, riser pressure drop, and measurement method (steady state vs. transient)

Source	Type I sum of squares	*df*	Mean square	*F*	Significance
Corrected model	42,258,627	7	6,036,947	1008.82	0.000
Intercept	168,396,041	1	168,396,041	28140.17	0.000
U_g	15,368,360	1	15,368,360	2568.16	0.000
Method	3630	1	3630	0.61	0.458
ΔP_{Riser}	23,447,385	1	23,447,385	3918.22	0.000
$U_g \times$ method	47,415	1	47,415	7.92	0.023
$U_g \times \Delta P_{Riser}$	2,988,577	1	2,988,577	499.41	0.000
Method $\times$ ΔP_{Riser}	378,533	1	378,533	63.26	0.000
$U_g \times$ method $\times$ ΔP_{Riser}	24,728	1	24,728	4.13	0.077
Error	47,874	8	5984		
Total	210,702,541	16			
Corrected total	42,306,500	15			

Computed using $\alpha = 0.05$ resulting in $R^2 = 0.999$ (adjusted $R^2 = 0.998$).

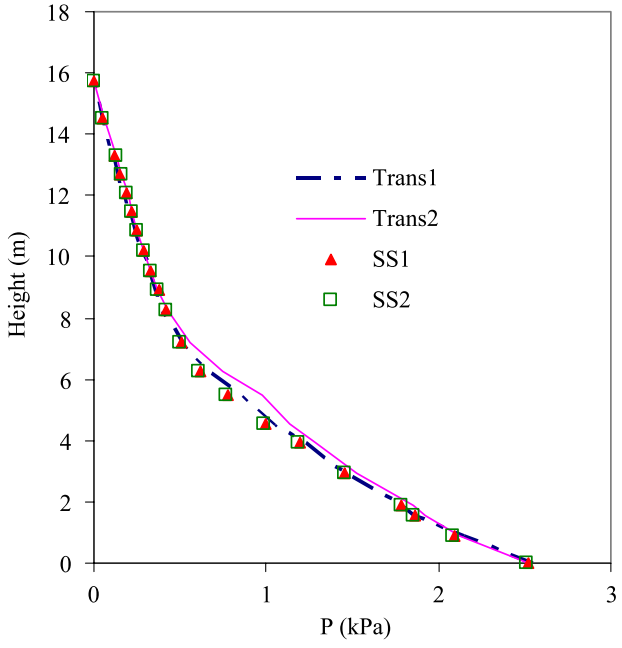

Fig. 11. Comparison in the axial pressure profile along the riser between the transient and steady state for $U_g = 2.75$ m/s at $\Delta P_{Riser} = 2.52$ kPa.

Typical axial pressure profiles are compared between the steady state and transient tests (Fig. 11). This comparison is for the case in which the riser was in the fast fluid bed regime. The duplicate tests agreed very closely; the root mean square (RMS) deviation was ± 2.1 Pa for the transient tests but only 0.024 Pa for the steady state tests. While the steady state tests were more repeatable, the deviation was three orders of magnitude smaller than the test values (0 to 2500 Pa, Fig. 11) and well within the required sensitivity to distinguish the primary features of the profile such as the height of the dense bed. A comparison of the transient against the steady state profiles generated an RMS deviation similar to that for the transient duplicates themselves, ± 3.2 Pa. The agreement between the transient and the steady state profiles was quite impressive. This is especially so considering that the data for the transient, covering all three operating regimes, was generated in under 20 min, while the steady state values required several hours of testing. The transient data itself was generated over a period of between 50 and 200 s depending upon the gas velocity. The transient method is capable of generating 10 to 40 riser profiles over different operating regimes. Thus, this method can provide tremendous time savings when attempting to identify operating regime features and transitions with only a small reduction in accuracy.

4. Summary

There is a controversy in literature on the range of velocities over which the different fluidization regimes exist, characteristics of each regime, and even on the existence of different transition velocities. A transient method is presented here which readily allows one to identify operational features and critical transition velocities. The riser was operated in fully dense transport regime prior to stopping the solids flow rate. The method was to measure the transient pressure drop across the riser during a solid flow cut-off experiment while maintaining a constant gas flow. This pressure drop was plotted against its time derivative to obtain a standard $\Delta P/\Delta L - G_s - U_g$ plot for characterizing operating regimes [1]. Instantaneous axial pressure profiles along the length of the riser were used to differentiate between dense ($\varepsilon = \text{constant} < 0.9$), fast fluidized (S- or C-shaped), and dilute regimes ($\varepsilon = \text{con-constant} > 0.95$). The time derivative of the pressure drop represents the solids flux at each point in time. The axial pressure profiles from the transient method agreed quantitatively with the steady state profiles.

The predicted solids fluxes during transient were compared with steady state values for given ΔP_{Riser} and U_g. The solids fluxes determined from both transient and steady state methods agreed very closely in fast fluidized and dense transport regimes. Statistical analysis demonstrated no significant difference for measurement method (steady state and transient main effect) on estimates of circulation rate at a given riser solids holdup. This, however, was not the case for the tail end of the cutoff decay curve for the dilute flow condition. The lack of accuracy in the dilute regime was conjectured to be due to the wide particle size distribution that resulted in segregation during the transient testing. Furthermore, this method did not rely on steady state measurements of pressure drops and solids flux that can be difficult when operating in the proximity of flow regime transitions due to hysteresis observed in CFB standpipes. This transient method offers an accurate, easy, rapid, and reproducible means of characterizing CFB operations over a wide range of flow conditions.

Symbols

g	Acceleration due to gravity (m^2/s)
G_s	Solids flux (kg/m^2 s)
t	Time (s)
U_g	Superficial gas velocity (m/s)
U_{mf}	Minimum fluidization velocity (m/s)
U_t	Terminal velocity (m/s)
z	Vertical coordinate (m)

Greek letters

ε	Voidage
ε_b	Bed voidage
ε_{mf}	Minimum fluidization voidage
ρ_b	Bed density (g/cm^3)
ρ_s	Solid density (g/cm^3)
ϕ	Sphericity
ΔP_{Riser}	Pressure drop across the riser (kPa)

Acknowledgements

The authors acknowledge the Department of Energy for funding the research through the Fossil Energy's Integrated Gasification Combined Cycle program. Operations of the CFB unit were made possible with support from Jim Devault, Alain Lui, and Todd Worstell.

References

[1] J. Yerushalmi, N.T. Cankurt, Powder Technol. 24 (1979) 187.
[2] C.S. Teo, L.S. Leung, Encyclopedia of fluid mechanics, in: N.P. Cheremisinoff (Ed.), Solids and Gas–Solids Flows, vol. 4, Gulf Pub., Houston, 1986, pp. 611–663.
[3] S.B.R. Karri, T.M. Knowlton, in: P. Basu, M. Horior, M. Hasatani (Eds.), Proceedings of the Third International Conference on Circulating Fluidized Beds, Pergamon, New York, 1991, p. 67.
[4] R.C. Zijerveld, F. Johnson, A. Marzocchella, J.C. Schouten, Powder Technol. 95 (1998) 185.
[5] H.T. Bi, L.S. Fan, Presented at AIChE Annual Meeting, Los Angeles, November, (1991). Paper No. 101E.
[6] H.T. Bi, J.R. Grace, Int. J. Multiph. Flow 21 (1995) 1229.
[7] K. Smolders, J. Baeyens, Powder Technol. 119 (2001) 269.
[8] D. Bai, K. Kato, J. Chem. Eng. Jpn. 28 (1995) 179.
[9] J. Li, L. Wen, W. Ge, H. Cui, J. Ren, Chem. Eng. Sci. 53 (1998) 3367.

[10] E.R. Monazam, L.J. Shadle, L.O. Lawson, Powder Technol. 121 (2001) 205.
[11] J.C. Ludlow, L. Lawson, L. Shadle, M. Syamlal, in: J.R. Grace, J. Zhu, H. de Lasa (Eds.), Circulating Fluidized Bed Technology VII, Canadian Society of Chemical Engineering, Ottawa, Canada, 2002, p. 513.
[12] Y. Li, M. Kwauk, in: J.R. Grace, J.M. Matsen (Eds.), Fluidization, Plenum, New York, 1980, p. 537.
[13] D. Kunii, O. Levenspiel, Powder Technol. 61 (1990) 193.
[14] J. Li, Modeling, in: M. Kwauk (Ed.), Fast Fluidization, Academic Press Inc., USA, 1994, p. 147.
[15] J.R. Grace, A.S. Issangya, D. Bai, H. Bi, J. Zhu, AIChE J. 45 (1999) 2108.
[16] M. Louge, H. Chang, Powder Technol. 60 (1990) 197.
[17] J.F. Perales, T. Coll, M.F. Llop, L. Puigjaner, J. Arnaldos, J. Cassal, in: P. Basu, M. Horio, M. Hasatani (Eds.), Circulating Fluidized Bed Technology III, Pergamon, Oxford, 1990, p. 73.
[18] K.-E. Wirth, Chem. Eng. Technol. 14 (1991) 29.
[19] L.J. Shadle, E.R. Monazam, J.S. Mei, in: J.R. Grace, J. Zhu, H. de Lasa (Eds.), Circulating Fluidized Bed Technology VII, Canadian Society of Chemical Engineering, Ottawa, Canada, 2002, p. 255.